A R C H I V E S O F M E T A L L U R G Y A N D M A T E R I A L S
Volume 58 2013 Issue 2
DOI: 10.2478/v10172-012-0187-0

W. WOŁCZYŃSKI*

THERMODYNAMIC PATTERN SELECTION IN THE STRIPES GENERATED PERIODICALLY DURING THE (Zn) – SINGLE CRYSTAL GROWTH

TERMODYNAMICZNA SELEKCJA MORFOLOGII PRĄŻKÓW GENEROWANYCH PERIODYCZNIE PODCZAS WZROSTU MONOKRYSZTAŁU (Zn)

The (Zn) – hexagonal single crystal growth was performed by the *Bridgman* system. Some eutectic stripes were generated periodically in the single crystal. The stripes consisted of the strengthening inter-metallic compound, $Zn_{16}Ti$ and (Zn) – solid solution. Two morphology transitions were recorded. At the first threshold growth rate, L-shape irregular rods transformed into regular lamellar structure. The transition was accompanied by the irregular into regular morphology alteration. The regular lamella into regular rods transition occurred at the second threshold growth rate. The new, proposed thermodynamic pattern selection criterion (PSC) of the lower minimum entropy production was applied to describe the structural transitions. The solid/liquid interface perturbation of the (Zn) – phase was referred to the marginal stability.

Keywords: minimum entropy production, marginal stability, surface tension anisotropy, structure selection, structure transformation

Heksagonalny monokryształ roztworu stałego (Zn) został wyprodukowany w układzie *Bridgmana*. Prążki eutektyczne zostały wygenerowane periodycznie w monokrysztale. Prążki składały się z umacniającego związku międzymetalicznego $Zn_{16}Ti$ oraz roztworu stałego (Zn). Zarejestrowano dwa przejścia morfologiczne. Przy pierwszej prędkości progowej nieregularne włókna o przekroju L doznały transformacji w regularne płytki. Temu przejściu towarzyszyła przemiana morfologii nieregularnej w regularną. Regularne płytki dokonały transformacji w regularne włókna przy drugiej prędkości progowej. Niższe minimum produkcji entropii to proponowane, nowe kryterium termodynamiczne dla selekcji struktur, jakie zastosowano by opisać przejścia strukturalne. Perturbacja frontu krystalizacji fazy (Zn) została odniesiona do stanu stabilności marginalnej.

1. Introduction

A strengthening phenomenon is often desired in some materials. Usually, the strengthening leads to significant increasing of some mechanical properties of a given material, [1], [2]. The hexagonal (Zn) – single crystal can be strengthened when is equipped with regular stripes which contain the $Zn_{16}Ti$ inter-metallic compound, [3]. Such a phenomenon was already known in some materials to which particles were added, [1], [2].

The studied hexagonal (Zn) – single crystal was doped by the small amount of titanium and copper. The addition of copper modifies the specific surface free energy at the solid /liquid interface. Copper does not form an inter-metallic compound with the zinc but is localized in the zinc / titanium solid solution, (Zn). However, titanium forms an inter-metallic compound with the zinc, $Zn_{16}Ti$. The (Zn) – $Zn_{16}Ti$ is the eutectic system. It provides an opportunity to control the growth of the Zn hexagonal single crystal, and first of all to control both an inter-striped spacing, F, shown in Fig. 1 and the stripe thickness, T, Fig. 2.

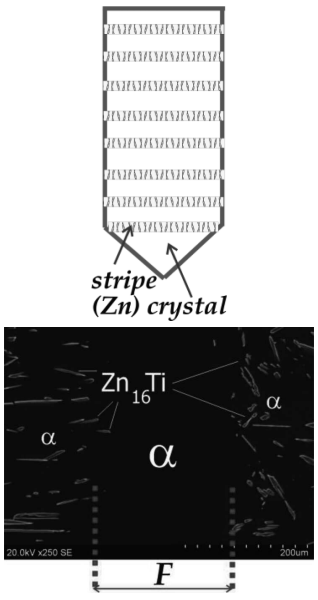

Fig. 1. Structure of the single crystal equipped with the stripes; a/ periodically localized stripes in a (Zn) – single crystal (scheme), b/ the F – inter-striped spacing; $(Zn) \equiv \alpha$

* INSTITUTE OF METALLURGY AND MATERIALS SCIENCE, 25 REYMONTA STR., 30-059 KRAKÓW, POLAND

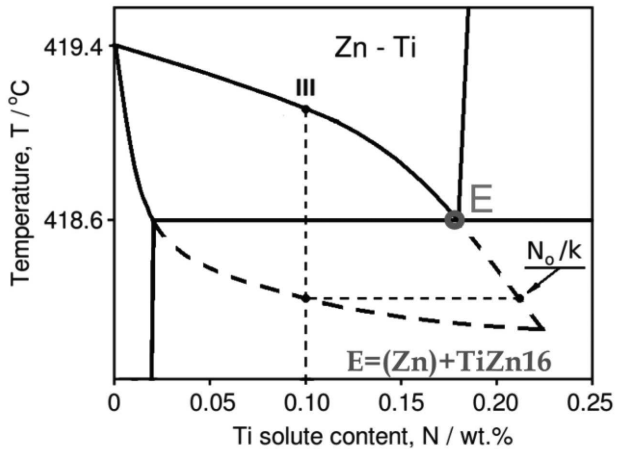

Fig. 2. Locations of the $III \equiv N_0$ – nominal solute concentration of Ti in the Zn-Ti phase diagram and equilibrium solidification path $III - E - N_0/k; N_E = 0.18$ $[wt.\%Ti]$, [4]; the ratio $F/T = (III-E)/(E-N_0/k)$ is satisfied for the equilibrium solidification

The full thermodynamic description of the (Zn) single crystal growth with periodic formation of the (Zn) – $Zn_{16}Ti$ stripes requires introduction the model that deals with the solute redistribution, [5], [6]. Next, there is also necessary to deliver a steady – state solution to the diffusion equation which yields the solute micro – field in the liquid at the eutectic s/l interface, [7]. The solution involves a proper localization of the thermodynamic equilibrium at the α/β inter-phase boundary together with the mechanical equilibrium situated just at the triple point of the s/l interface. This solution also allows considering the entropy production in such a system within which the transition from lamellar into rod-like microstructure occurs, [8]. The behaviour of the Ti – solute redistribution along the (Zn) – single crystal matrix, (F – area) and a stripe's structure selection will be analyzed in the current model. The new principle (PSC) of the lower minimum entropy production, [9] will be applied in the analysis. The branching phenomenon observed for the rod-like structure formation will be treated as a bifurcation and referred to marginal stability.

2. Solute redistribution in the (Zn) – matrix

In the case of the (Zn) – single crystal which contains strengthening stripes, Fig. 1a, the Ti – solute redistribution can be measured along the (Zn) – matrix (within the F - area), Fig. 1b. The applied *Bridgman* furnace was working in the experiment as a closed system. Thus, the control of strengthening could be done, to some extent, by an adequate choice of a nominal concentration of titanium and by applying a proper growth rate, v, on which the $\alpha(v)$ back-diffusion parameter depends. The solute redistribution is the function of mentioned $\alpha(v)$ back-diffusion parameter, [6].

The choice of the nominal solute concentration results in the stripe thickness. The smaller the distance between nominal solute concentration and the eutectic point on the *liquidus* line is, the wider are the stripes, Fig. 3. The solidification occurs along the solidification path cyclically, and precipitates are rejected at the end of each cycle to form the stripes, Fig. 3.

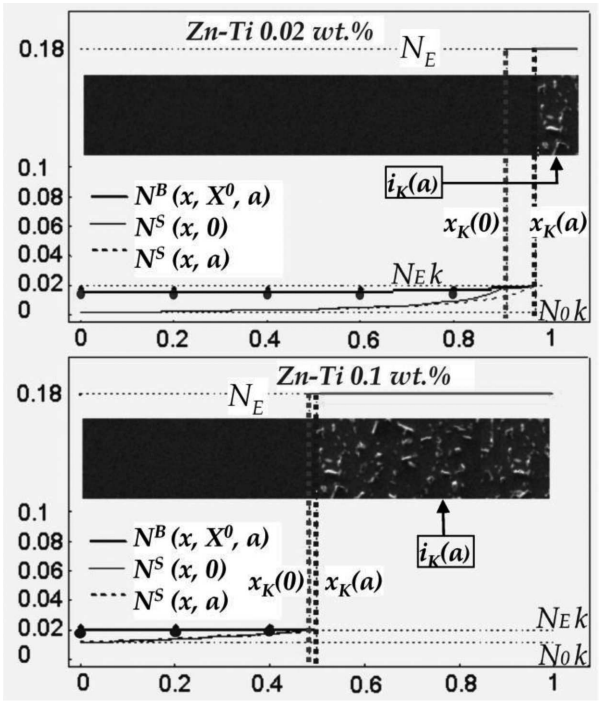

Fig. 3. Ti – solute redistribution as calculated for two alloys of the nominal Ti – solute concentration equal to: 0.02 $wt.\%$ and 0.1 $wt.\%$, respectively, [10], $N^S(x,\alpha) = k\,N^L(x,\alpha)$; the Zn-Ti single crystals were produced at the Faculty of Non-Ferrous Metals of AGH University of Science and Technology, Kraków

The $N^B\left(x; X^0, \alpha\right)$ – function, delivered theoretically, fits well the measurement points within the F – area for both examined samples, Fig. 3. The $N^B\left(x; X^0, \alpha\right)$ – function describes the solute redistribution after back-diffusion, [6].

$$N^B\left(x; X^0, \alpha\right) = \left[k + \beta^{ex}\left(x; X^0\right)\,\beta^{in}\left(X^0, \alpha\right)\right]\,N^L(x; \alpha) \quad (1)$$

k– partition ratio, $[mole\ fr./mole\ fr.]$; x – crystal amount, [dimensionless]; $x = X^0$ – crystal amount at arrested growth; β^{ex} – coefficient of redistribution extent, [dimensionless]; β^{in} – redistribution intensity coefficient, [dimensionless]; N^L – liquid content, $[mole\ fr.]$; Eq. (3).

$$N^L(x; \alpha) = N_0\ (1 + \alpha\ k\ x - x)^{(k-1)/(1-\alpha k)} \quad (2)$$

$$\alpha = D_S\ t_l\ F^{-2} \quad (3)$$

D_S– diffusion coefficient into the solid, $\left[m^2/s\right]$; t_l – time necessary for the F – matrix formation, $[s]$.

As mentioned, the crystal growth is accompanied by the eutectic precipitates. The growth rate, imposed in the *Bridgman* system for a single crystal growth (with a seed) $v > 0$, does not involve the equilibrium solidification. Thus, the solidification path is longer than that shown in Fig. 2. Therefore, it was possible to obtain precipitates even for the nominal solute concentrations: $N_0 = I = 0.01$ $[wt.\%Ti]$, $N_0 = II = 0.02$ $[wt.\%Ti]$, when the imposed growth rate, v, involves the solidification path elongation beyond the eutectic point till the N_K – point on the *liquidus* line. N_K is the solute content in the liquid at the end of solidification.

The ratio between an amount of the crystal, x_K, and an amount of precipitate, i_K, depends on the mentioned solidification path elongation beyond the eutectic point:

$$x_K/i_K = (N_E - N_0)/(N_K(\alpha, N_0) - N_E) \quad (4)$$

The end of solidification path is: $N_K(\alpha, N_0) = N^L(x_K, \alpha)$, and x_K is defined as follows:

$$x_K(\alpha, N_0) = \frac{1}{1-\alpha k}\left[1 - (N_E/N_0)^{\frac{1-\alpha k}{k-1}}\right] \text{ when } 0 \leqslant \alpha \leqslant \alpha_E(N_0) \tag{5a}$$

$$x_K(\alpha, N_0) = 1 \text{ when } \alpha_E(N_0) < \alpha \leqslant 1 \tag{5b}$$

with $(\alpha_E\, k)^{\frac{k-1}{1-\alpha_E k}} = N_E/N_0$, [6].

Regarding to the above considerations, $i_K(\alpha, N_0) = 1 - x_K(\alpha, N_0)$, [dimensionless].

3. Strengthening phase protrusion

The recent solution to the diffusion equation assumes the existence of the mechanical equilibrium at the tripe point of the s/l interface and thermodynamic equilibrium along the inter-phase boundary, [7]. The steady-state solution to the diffusion equation is given separately for the both eutectic lamellae: α - phase lamella, and β- phase lamella. So,

a/ for the α - eutectic phase formation (the (Zn) – phase in the Zn – Ti system),

$$\delta C(x,z) = \sum_{n=1}^{\infty} A_{2n-1} \cos\left(\frac{(2n-1)\pi x}{2S_\alpha}\right) \exp\left(-\frac{(2n-1)\pi}{2S_\alpha} z\right) \tag{6}$$

$$A_{2n-1} = -\frac{4}{(2n-1)\pi} \int_0^{S_\alpha} f_\alpha(x) \cos\left(\frac{(2n-1)\pi x}{2S_\alpha}\right) dx \quad n = 1,\ 2, \ldots \tag{6a}$$

b/ for the β – eutectic phase formation (the $Zn_{16}Ti$ – phase in the Zn – Ti system), α

$$\delta C(x,z) = \sum_{n=1}^{\infty} B_{2n-1} \cos\left(\frac{(2n-1)\pi (x - S_\alpha + S_\beta)}{2S_\beta}\right) \exp\left(-\frac{(2n-1)\pi}{2S_\beta} z\right) \tag{7}$$

$$B_{2n-1} = -\frac{4}{(2n-1)\pi} \int_{S_\alpha - S_\beta}^{S_\alpha} f_\beta(x) \cos\left(\frac{(2n-1)\pi (x - S_\alpha + S_\beta)}{2S_\beta}\right) dx \tag{7a}$$

$C-$ solute concentration within the micro-field formed in the liquid,[$at.\%$]; S_j – half the width of the eutectic phase lamellae, [m], respectively; f_j – function used in the boundary condition formulation for the α and β – eutectic phases formation, [$at.\%$], ($j = \alpha, \beta$), respectively; x, z – geometrical coordinates, [m]; $\delta C(x,z)$ – difference between $C(x,z)$ and C_E, where C_E is the eutectic concentration of the solute.

The above solution ensures the satisfaction of the local mass balance, Eq. (8). However, the strengthening phase protrusion, d, is to be taken into account, Fig. 4.

$$\int_0^{S_\alpha} \delta C(x,0)\, dx + \int_{S_\alpha}^{S_\alpha + S_\beta} \delta C(x,d)\, dx = 0 \tag{8}$$

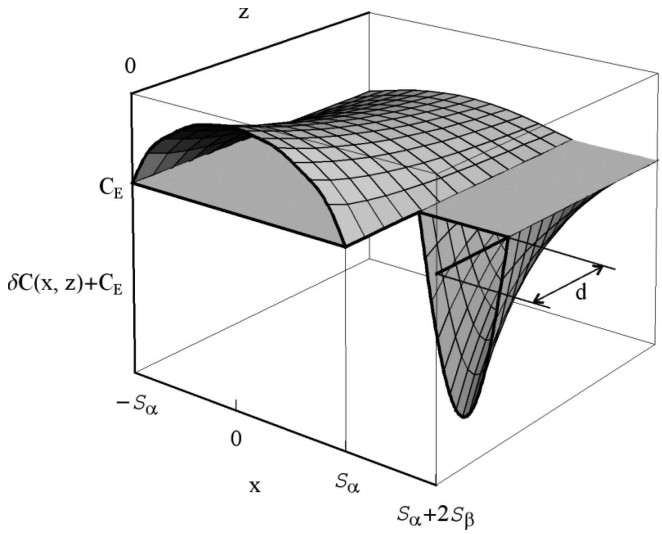

Fig. 4. Local mass balance within the solute concentration micro-field for an eutectic system

The protrusion of the eutectic leading phase (strengthening phase), predicted theoretically, Fig. 4, and observed experimentally in the past, [11], has also been revealed within the stripes which contain the ((Zn) + $Zn_{16}Ti$) eutectic, Fig. 5.

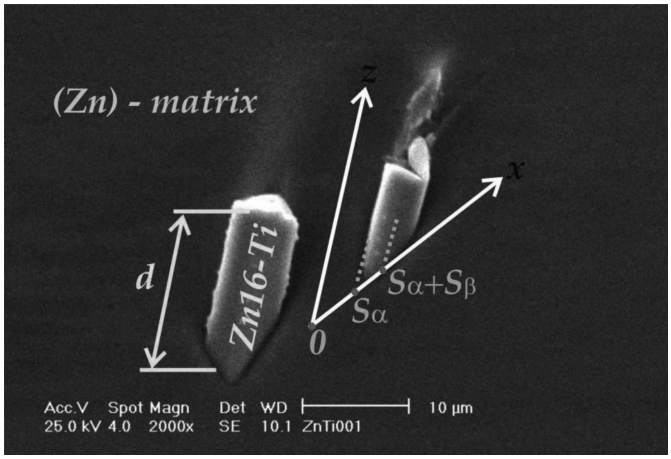

Fig. 5. The $Zn_{16}Ti$ phase protrusion revealed in the stripes (the EDS observation); the x, z – coordinate system presents the localization of the Ti – solute concentration micro-field; the d – leading phase protrusion is defined due to the (Zn) – single crystal growth arresting

4. Thermodynamic selection of the eutectic pattern

The only condition which defines the stationary state is the criterion of minimum entropy production, [12]. The entropy production per unit time, P_S^D, $S = R, L$, is calculated as follows, [13]:

$$P_S^D = \int_V \sigma\, dV \quad \sigma = R^*\, \varepsilon\, C^{-1}\, (1-C)^{-1}\, D\, \nabla^2 C \tag{9}$$

V is the so-called „thermodynamic macroscopic point" inside of which all essential fluxes are observed, [14]; R^* – gas constant, [$J/(mole\ K)$]; ε – thermodynamic factor, [dimensionless]; C – solute content, [$at.\%$]; σ – entropy production per unit time and per unit volume, $\left[mole\ fr.^2/\left(m^3 s\right)\right]$.

The entropy production for a rod-like and lamellar structure formation is, respectively:

$$P_R^D = V_1\, v\, \left(r_\alpha + r_\beta\right)^{-1} + V_2\, v\, \left(r_\alpha + r_\beta\right)^{-2} + V_3\, v^2 + V_4\, v^2\, \left(r_\alpha + r_\beta\right) + V_5\, v^3\, \left(r_\alpha + r_\beta\right)^2 \quad (10a)$$

$$P_L^D = W_1\, v\, \left(S_\alpha + S_\beta\right)^{-1} + W_2\, v\, \left(S_\alpha + S_\beta\right)^{-2} + W_3\, v^2 + W_4\, v^2\, \left(S_\alpha + S_\beta\right) + W_5\, v^3\, \left(S_\alpha + S_\beta\right)^2 \quad (10b)$$

in respect to the solution to Eq. (9). $V_n; W_n n = 1, ..., 5$ – constants contain material parameters, [15]; $r_j, (j = \alpha, \beta)$ – size of the matrix and rod radius within the regular rod-like structure, respectively.

The calculations of the entropy production applied to the Zn-Ti system are connected with the following experimental observations: for $0 < v < v_1$, L-shape rods equipped with branches appear, (irregular structure), for $v_1 < v < v_1^{'}$, L-shape rods with disappearing branches and regular lamellae coexist, for $v_1^{'} < v < v_2$, regular lamellae are formed, exclusively, for $v > v_2$, regular rods are formed, exclusively.

The appearance of the observed structure is accompanied by a proper entropy production, as postulated. Since the considered solidification occurs under stationary state, therefore the entropy production, P_D, manifests its minimum, Fig. 6. The calculations are made to describe the competition between two eutectic regular structures formation (lamellar and rod-like structure formation).

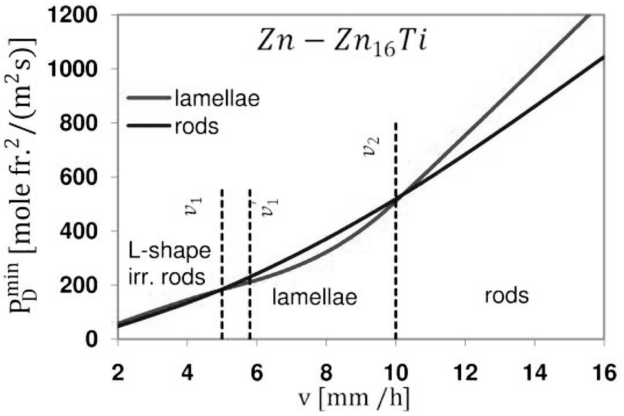

Fig. 6. Comparison of minimal values of the entropy production calculated for both regular rod-like structure formation (formed twice) and regular lamellar structure formation

The calculations of the entropy production, P_S^D, applied to the Zn-Ti system are made with an implementation of the model for rotation of the mechanical equilibrium around the triple point of the s/l interface. The mechanical equilibrium is established by the parallelogram of the anisotropic specific surface free energies together with inter-phase boundary free energy.

The rotation is performed in function of the increasing growth rate and adequate changes of the s/l interface curvature of the non-faceted (Zn) – phase, Fig. 7.

As a result of the varying growth rate, the s/l interface curvature changes due to rotating crystallographic orientation. $\sigma_{(Zn)}^L$ – specific surface free energy for (Zn) – phase, $\left[J/m^2\right]$; $\sigma_{(Zn)-Zn16Ti}^L$ – inter-phase boundary free energy, $\left[J/m^2\right]$.

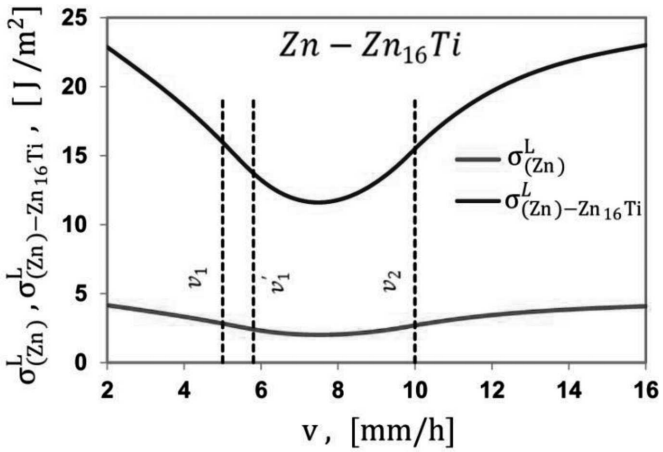

Fig. 7. Changes of the specific surface free energy, $\sigma_{(Zn)}^L$, and the inter-phase boundary free energy, $\sigma_{(Zn)-Zn16Ti}^L$, as applied to the calculation of the $V_n; W_n n = 1, ..., 5$ – coefficients

5. Irregular eutectic growth

Thermodynamics of the eutectic s/l interface formation has already been developed to some extent, [16], [17], [18]. It postulates that the regular structure areas exist inside the generally irregular morphology, as observed within the growth rates range, $0 < v < v_1$. Thus, two characteristic spacing can be selected within the generally irregular rod-like eutectic morphology: a/ the R – spacing which is associated with the regular rod-like structure formation; this spacing is referred to the criterion of minimum entropy production, which describes the stationary state, Fig. 8, and b/ the λ_s^i – spacing which corresponds to the maximal destabilization of the non-faceted (Zn) -phase s/l interface, Fig. 9; this perturbation wave, λ_s^i, is referred to the state of marginal stability which is created at that time of structure formation.

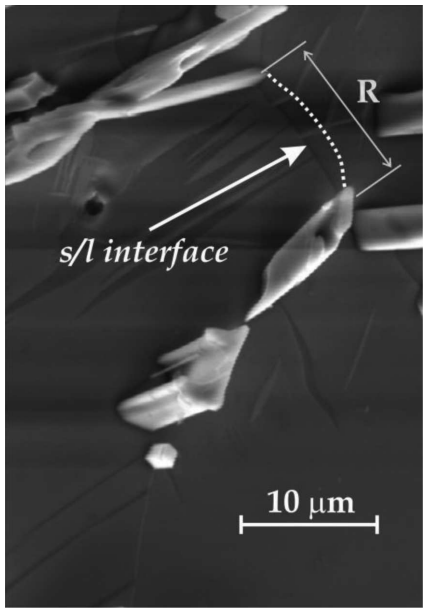

Fig. 8. Selection of the R – spacing by the minimum entropy production; frozen s/l interface has a typical parabolic shape; $R = 2\left(r_\alpha + r_\beta\right)$

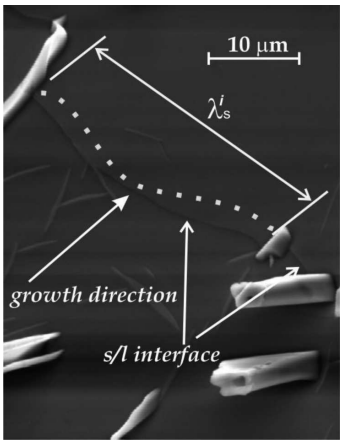

Fig. 9. Selection of the λ_s^i – spacing by the state of marginal stability; frozen s/l interface is visible as a wave of perturbation

Both states (stationary and marginal stability) can be localized on the surface of the entropy production paraboloid, [13], [14], [17] as plotted for steady-state solidification by the *Bridgman* system, Fig. 10.

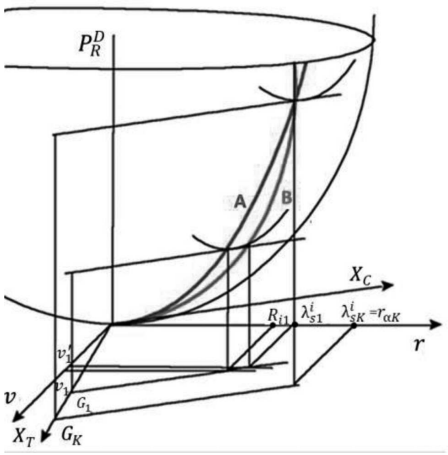

Fig. 10. Localization of the A – trajectory representing stationary state and B – trajectory defining marginal stability for the irregular rod-like eutectic growth

X_C – generalized thermodynamic force associated with the mass transport, [*at.%/m*]; X_T – generalized thermodynamic force associated with the heat transfer; [*K/m*]; v – crystal growth rate, [*m/s*]; λ – inter-lamellar spacing within the regular eutectic structure, [*m*].

Two trajectories are plotted in the Fig. 10: a/ A – trajectory of local minima of the paraboloid for regular eutectic structure formation, shown in Fig. 8, /B – trajectory of the marginal stability which is referred to the maximal destabilization of the s/l interface, shown in Fig. 9 connected to the branching phenomenon (bifurcation). The oscillation occurs between both trajectories as shown for a given condition of solidification, v_1, G_1, when generally irregular eutectic structure is formed.

Received: 20 January 2013.

6. Concluding remarks

According to the current model, this eutectic structure appears within the strengthening stripe which is the winner in a thermodynamic competition (which has its minimum situated lower), Fig. 6. So, the lower localized minimum entropy production is a pattern selection criterion successfully applied to determine the winner in the structural competition, Fig. 6. The postulated principle is valid even when the irregular eutectic structure growth occurs.

Acknowledgements

The financial support from the Polish Ministry of Science and Higher Education (MNiSW) under contract N N 508 480038 is gratefully acknowledged.

REFERENCES

[1] R. Ebeling, M.F. Ashby, Philosophical Magazine **13**, 805-834 (1966).
[2] N. Zarubova, B. Sestak, Physica Status Solidi **30**, 365-374 (1975).
[3] G. Boczkal, Chapter 7 in the book: Modern Aspects of Bulk Crystal and Thin Film Preparation, Rijeka – Croatia, 141-162 (2012), ed. In Tech, eds N. Kolesnikov & E. Borisenko.
[4] J. Murray, Zn-Ti Phase Diagram for Stable Equilibrium, in: T. Massalski (Ed.), Binary Alloy Phase Diagrams, ASM International, (1990), Park Ohio, USA.
[5] H.D. Brody, M.C. Flemings, Trans AIME **236**, 615-624 (1966).
[6] W. Wołczyński, Chapter 2 in the book: Modelling of Transport Phenomena in Crystal Growth, Southampton, UK – Boston, USA, 2000, ed. WIT Press, eds J.S. Szmyd & K.Suzuki.
[7] W. Wołczyński, Defect and Diffusion Forum **272**, 123-128 (2007).
[8] W. Wołczyński, International Journal of Thermodynamics **13**, 35-42 (2010).
[9] W. Wołczyński, Chapter 9 in the book: Modern Aspects of Bulk Crystal and Thin Film Preparation, ed. In Tech, (2012), Rijeka, Croatia, eds N. Kolesnikov, E. Borisenko.
[10] G. Boczkal, B. Mikułowski, W. Wołczyński, Materials Science Forum **649**, 113-118 (2010).
[11] V.L. Davies, Journal of the Institute of Metals **93**, 10-14 (1964).
[12] I. Prigogine, Introduction a la Thermodynamique des Processus Irreversible, Monographies DUNOD, Paris, France, 1968.
[13] S. Kjelstrup, D. Bedeaux, Non-Equilibrium Thermodynamics of Heterogeneous Systems. World Scientific Pulishing Co. Ltd., M. Rasetti, New Jersey – USA, London – UK, Singapore, Beijing – China, Shanghai – China, Hong Kong, Taipei – Taiwan, Chennai – India, 2008.
[14] P. Glansdorff, I. Prigogine, Thermodynamic Theory of Structure, Stability and Fluctuations, John Wiley & Sons, London, UK – New York, USA – Sydney, Australia – Toronto, Canada, 1971.
[15] W. Wołczyński, B. Billia, Materials Science Forum **215/216**, 313-322 (1996).
[16] D.J. Fisher, W. Kurz, Acta Metallurgica **28**, 777-794 (1980).
[17] W. Wołczyński, Materials Science Forum **215/216**, 303-312 (1996).
[18] W. Wołczyński, R. Cupryś, B. Major, Archives of Metallurgy and Materials, (previously Archives of Metallurgy) **43**, 309-317 (1998).